In-place determination of topsoil shear properties for mobility study

Ph Gotteland, O Benoit, O Ple

In-place determination of topsoil shear properties for mobility study

Ph. GOTTELAND [(1)], O. BENOIT [(1)], O. PLE [(1)]*

[(1)] Laboratoire Interdisciplinaire de Recherche Impliquant la Géologie et la Mécanique (Lirigm), Université de Grenoble, BP 53 - 38041 Grenoble Cedex 9 France

** presenting author: Dr Philippe GOTTELAND - E-mail: philippe.gotteland@ujf-grenoble.fr*
Tel.: +33476828080 - Fax: +33476828070

Abstract

A prototype experimental device was developed to perform shear tests by translation of a charged plate on soil at slow speed representative of soil mechanics tests, or fast speed representative of the slip kinetics of a vehicle's running gear. The soil tested was clean sand with frictional behaviour. In order to identify the failure mechanism, the shear test was numerically simulated with DEM modelling. The mechanism identified showed a failure located on juxtaposed and successive slip lines. The analytical simulation of this mechanism makes it possible to calculate its geometry by analogy with the experimental results and to identify the mechanisms involved in the sinkage induced by shearing.

1. Introduction

The movement of a vehicle on a soil induces two types of opposite forces. In off-road conditions, the running gear, composed of tracks or wheels, sinks into the surface soil and encounters obstacles which cause a resistance to the movement. At the same time, it provides a tractive effort making it possible for the vehicle to advance. This effort results from the transmission of the engine torque to the soil. The study of these resistant and driving forces is necessary to model the mobility of a vehicle.
Within an investigation of a global mechanical device for mine clearance [1], full-scale tests were carried out on various soils to identify the mechanisms influencing the mobility of a vehicle and to validate the models developed. In order to reproduce and to study the two principal mechanisms, a prototype experimental device was developed allowing sinkage tests and translation shear tests [2]. This can be effective to model the tractive effort of a vehicle provided that the phenomena brought into play are well understood.
This article reports the validation of the translation shear test for the study of granular top soil shearing. After review on shearing and its influence on the mobility of a vehicle, the experimental study is presented: the prototype device allowing the translation shear tests and the granular soil tested. The results are presented and phenomena are modelled to understand the soil's failure mechanism.

2. Shear tests and their interpretations

The shearing of the soil causes it to fail, a phenomenon that has generated great interest on the part of the scientific community in shear tests and their interpretation. Various types of laboratory and in-situ soil-shearing tests exist. Laboratory tests have the advantage of being conducted in well-controlled conditions. As the in-situ tests are carried out on in-situ materials, the problems of handling materials and modifying the soil's mechanical characteristics are restricted.
The most common laboratory tests are direct shear tests and triaxial compression tests. The direct shear test consists in confining a soil sample in a box divided into two parts by a horizontal plane (Figure 1a). A normal load is applied to the sample and a horizontal displacement is imposed on one of the two parts of the shear box. The triaxial compression

test consists in applying a radial stress and a longitudinal stress of different combinations to a drained or undrained cylindrical sample (Figure 1b).
Many in-situ tests exist: the in-situ direct shear test, the shear vane test, the vane-cone test, the annular shear test and the translation shear test. The in-situ direct shear test makes it possible to study undisturbed soil. It consists of a delicate operation of "cutting" a soil sample in order to place the device around it [3]. The shear vane test [4] is a tool with four vertical wings sunk into the soil with a rotation (Figure 1c). The torque to obtain the failure of the soil on a cylindrical surface around the wings gives the shear force. This tool is usable only in fine materials because it is impossible to vary the normal load. The penetrometer vane-cone [5] combines two measurements: the penetration resistance of the conical penetrometer and the shearing of the shear vane test (Figure 1d). The vane-cone is inserted in the soil and then undergoes a rotation at a given depth. This test allows one to study the mobility of vehicles on clay soils [6]. The annular shear test (Figure 1e) consists in the rotation at a constant speed of a loaded ring with a smooth interface or with grousers. This test is often used to estimate the soil shearing for mobility studies [7] [8]. The translation shear test (Figure 1f) consists in the translation at a constant speed of a loaded plate with a smooth interface or with grousers. This test is also used for mobility [9].

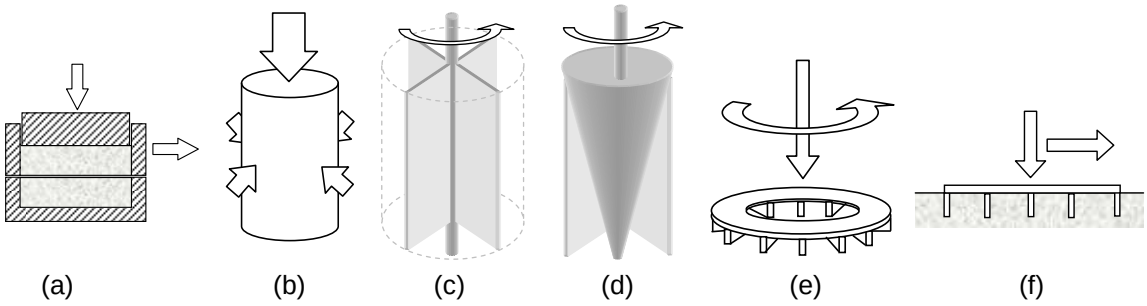

Figure 1. Examples of shear tests: (a) direct shear test, (b) triaxial compression test, (c) shear vane test, (d) vane-cone test, (e) annular shear test, (f) translation shear test

The shear stress τ according to displacement *j* generally shows a curve with or without a peak of stress τ_{pic} followed by the critical state τ_m (Figure 2), which are characteristic of soil failure. The peak state depends on the bulk unit weight of the soil: typically a dense sand has a behaviour with a peak state contrary to a loose sand.

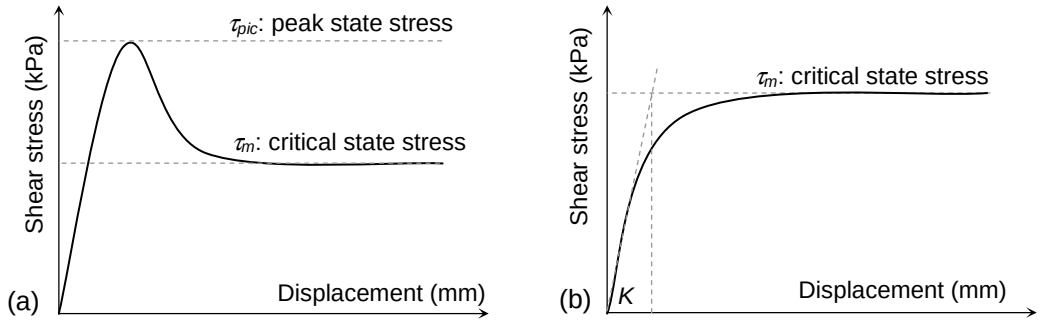

Figure 2. Shear-displacement curves *(a) with a peak state, (b) without a peak state*

To determine the tractive effort of a vehicle, it is necessary to model the shear-displacement curve on the entire displacement field. This has been modelled in several ways, depending on whether the curve has a peak or not.
For soils with a peak state, the relationships most often used are Bekker's [10] [11] , Oïda's [12] and Wong's [13]. For the soils without a peak state, the relationship used is Janosi's [14]. Shear stress τ can be determined by the theoretical interpretation of the tests using the

concept of yield criterion. The most frequently used is the Mohr-Coulomb yield criterion ($\tau = \sigma \tan \Phi + c$) characterized by two parameters: the friction angle ϕ and cohesion c. In the field of vehicle mobility, the shear test most frequently used is the annular shear test. When the annular shear test is carried out with several normal loads, Coulomb's parameters can be determined [15]. However, the failure of the soil below the ring can appear on an oblique surface compared to that of the ring. In this case, the values of normal load and shear are unknown along the failure surface [16] and determining c and ϕ is very complex. This phenomenon can be prevented by applying an overload around and inside the ring [17].

3. Experimental methods and soil tested

3.1. Experimental device

In order to reproduce the mechanisms associated with soil shearing by the running gear, a prototype experimental device was developed [18] providing a shear test by the translation of a plate (Figure 3).

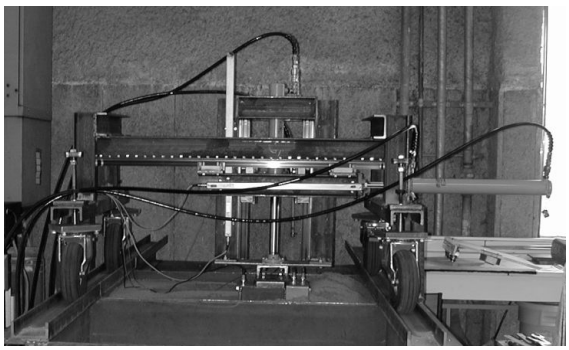

Figure 3. Translation shear test with the prototype experimental device

This test is carried out with the translation on approximately 400 mm, at a slow constant speed (~23 $mm.min^{-1}$) or fast (~14 $mm.s^{-1}$), with an instrumented shear head (Figure 4) loaded vertically. The device consists of a fixed frame on which a mobile frame moves for horizontal and vertical movement. The mechanical translations are controlled by guides with rollers sliding on rails, thus preventing any rotation. Horizontal jack is used in traction and has a maximum stroke of 600 mm. Vertical jack is used in compression and has a maximum stroke of 400 mm. Their maximum capacity is 25 kN. Five parameters are measured simultaneously: horizontal displacement j, vertical displacement (sinkage) z, vertical load N, total horizontal force T_{total}, bulldozing force T_{bull},
The shear force T is calculated as the difference between the total horizontal force and bulldozing force ($T = T_{total} - T_{bull}$) .
Horizontal and vertical displacements are measured. The shear plate (length L = 340 mm, width l = 240 mm) can have a smooth interface to represent the soil-steel friction, an alveolate interface to confine the soil and reproduce a soil-soil friction, and an interface with grousers to study their influence.

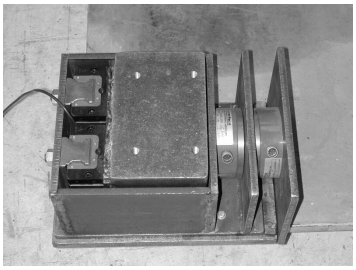

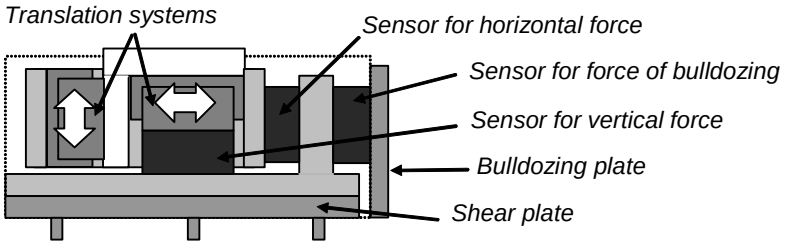

Figure 4. Instrumented shear head

3.2. Tested soil and experimental protocols

The translation shear tests were carried out on 0/5-mm sand. Extracted underwater, it has less than 0.3% fine particles (particle sizes <80 mm) and 85% of particles smaller than 2 mm. Its low fines content makes it insensitive to water. The primarily siliceous grains are angular. The French GTR classification [20] of this sand is D1. The mechanical characteristics of the D1 sand were measured by three triaxial compression tests and three direct shear tests. The angle of friction ϕ is 33° with a variability Δ of 6% and the cohesion is close to 0 (<1 kPa). The behaviour of this sand can be considered as purely frictional.

For the presented translation shear tests, the device is fixed on a 1-m^3 bin (height 0.8 m, width 1 m, length 1.3 m). The sand set-up is defined by a protocol so that the bulk density can be reproduced. This protocol consists in filling the bin in four 200-mm-thick layers compacted with energy of 50 $J.m^{-2}$ (weight of 23 kg falling twice at a distance of 0.4m on an impact surface of approximately 0.02 m^2). The average bulk unit weight obtained on 24 bins is 16.3 $kN.m^{-3}$ (variability of 5%). The water content was also controlled by four samples per layer that were dried and weighed (average value is 1.2% with a variability of 6%, Table 1).

Table 1: Properties of D1 sand

D1 sand	Properties	Mean value	Variability Δ
Mechanical characteristics (triaxial tests, direct shear tests)	Friction angle ϕ	33°	6%
	Cohesion c	<1 kPa	-
(translation shear tests)	Water content w	1.2%	6%
	Bulk unit weight γ	16.3 $kN.m^{-3}$	5%

3.3. Experimental results

Two phenomena were studied: the relationship between the normal load N and the shear force T, and the sinkage of the instrumented shear head induced by the shearing of the D1 sand. Twenty-four translation shear tests were carried out on sand, four per modality. The shear plate used was the alveolate plate to reproduce a soil-soil friction necessary for determining the mechanical parameters of the sand. The normal loads N tested were 4.1 kN, 8.2 kN and 12.3 kN (normal stress σ = 50, 100 and 150 kPa, respectively). The force-displacement curves and the sinkage-displacement curves showed good reproducibility (Figure 8), confirming the relevance of the protocol's set-up. The curve of the average values for the shear forces had a variability Δ of 5%. It showed a shape without a peak state. The curve of the average values for the induced sinkage had a variability Δ of 7%. Quasi-linear until approximately 50% of relative displacement j/L, it showed a slight inflection for the higher values. The same shape of the average curves was found for the other normal loads and translation speeds (Figure 5).

The slope Γ at the origin of the curve (j/L, T) characterizes the initial part of the curve. The shear force T_{20} to 20% of relative displacement is representative of the value of the critical state force. The relative sinkage z_{20}/L to 20% of relative displacement explains the phenomena induced by the shearing of the soil. The average values for each parameter are also presented with their total variability. These results show that the variation of the normal load N influenced the three parameters. The increase in the normal stress σ caused an increase in the initial slope Γ, the critical state force T_{20} and the relative sinkage z_{20}/L. Changing the translation speed influenced the initial slope Γ of the curves (j/L, T) (Figure 6). For the shear tests at slow speed (23 $mm.min^{-1}$), the initial slope was more significant than for the shear tests at fast speed (14 $mm.s^{-1}$). The ratio between the two slopes was approximately 5 whatever the normal load. The critical state force T_{20} and the relative sinkage z_{20}/L were not affected by the translation speed in the range tested.

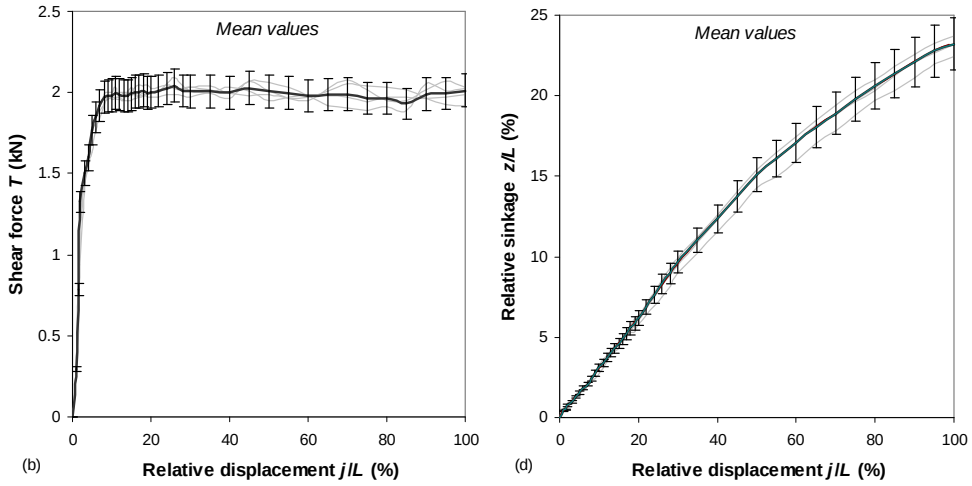

Figure 5. Translation shear test, (alveolate plate, normal stress σ = 50 kPa, slow speed = 23 mm.min^{-1} (b) mean values (j/L, T) curve (Δ = 5%), (d) mean values (j/L, z/L) curve (Δ = 7%)

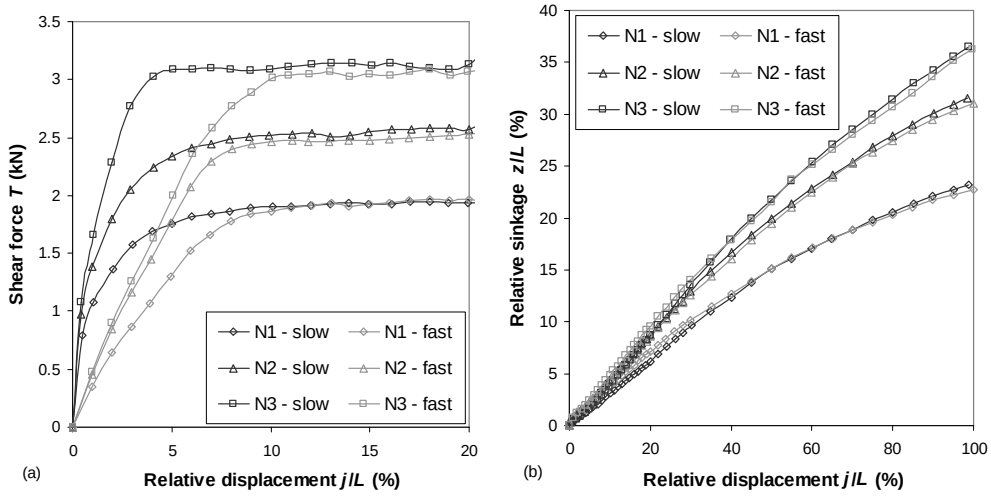

Figure 6. Influence of the translation speed (slow speed = 23 mm.min^{-1}, fast speed = 14 mm.s^{-1}) during shear tests with alveolate plate (normal load N1 = 50 kPa, N2 = 100 kPa, N3 = 150 kPa) on D1 sand (a) mean values (j/L, T) curves, (b) mean values (j/L, z/L) curves

4. Numerical simulation

4.1. Simulation description

In order to visualize the failure mechanisms involved in the translation shear tests on a granular soil, numerical simulations were carried out with a program based on the Discrete Element Method (DEM). This method allows one to view a granular material as a collection of solids, rigid or not, interacting at their contact points, with or without friction. The position and the velocity of each grain in the sample are then calculated at each time step by solving the dynamics equations [21]. Numerous programs were developed. The program used in this research is based on a particular DEM, called Contact Dynamics (CD) [22] [23]. In the two-dimensional simulations reported below, the soil is modelled as a collection of convex polygonal grains initially in equilibrium under gravity in a rectangular box (length = 400 mm, height = 150 mm) with main characteristics shown in Table 2.

Table 2. Sample parameters

Number of grains	4598
Control radii of grains (mm)	$2 \leq r \leq 2.7$
2D density of grains (g/cm^2)	$\rho = 2.4$
Initial void ratio	$e_0 = 0.193$
Friction coefficient between the grains	$\mu = 0.5$
Limit conditions: walls friction coefficient	$\mu_{lim} = 0$
Steel-soil friction coefficient	$\mu_{local} = 0.364$
Normal and tangential restitution coefficients	$e_N = 0.2$, $e_T = 0.1$

For comparison with experiments, three kinds of tools (length = 100 mm, height = 25 mm) were modelled. The simplest was a smooth rectangular plate. A rough plate was also simulated by gluing a layer of polygonal grains onto the lower face of the smooth plate. Various plates with grousers were tested with two and three grousers 10 mm high. The same local friction coefficient μ_{local} = 0.364 was chosen for the smooth plate as for those with grousers (such as soil-steel friction), but the friction coefficient of the rough plate was equal to 0.5, the same as the grain-to-grain interaction, in order to model a soil–soil friction.
A constant vertical load and a constant horizontal velocity were both applied to the tool. Two forces (N = 2.5 N and N = 5 N) and two translation speeds (V = 1 cm.s^{-1} and V = 0.1 cm.s^{-1}) were tested. Since a tool is a rigid assembly of grains, the program makes it possible to determine the resultant forces that take place in the different parts of the tool. In these two-dimensional simulations, this was also particularly useful to remove the force component T_{bull} due to the pad accumulation in front of the tool to obtain the shear stress T as defined.

4.2. Numerical results

The conditions during the simulation are relatively distant from those of the laboratory tests: the numerical simulations are two-dimensional, the ratio between the dimension of the plate and the diameter of the grains leads to a low number of grains in contact with the tool and the pressures on the tool are low. However, modelling aimed to provide qualitative comparisons with the tests carried out on D1 sand, in particular in terms of the evolution of the shearing and the sinkage of the plate. Moreover, the shape of the shearing-displacement curves and the sinkage-displacement curves obtained from numerical simulations were very similar (Figure 7) to the experimental tests (Figure 6). The fluctuations of the numerical curves were caused by the discrete and heterogeneous nature of the grains and their necessarily limited number.

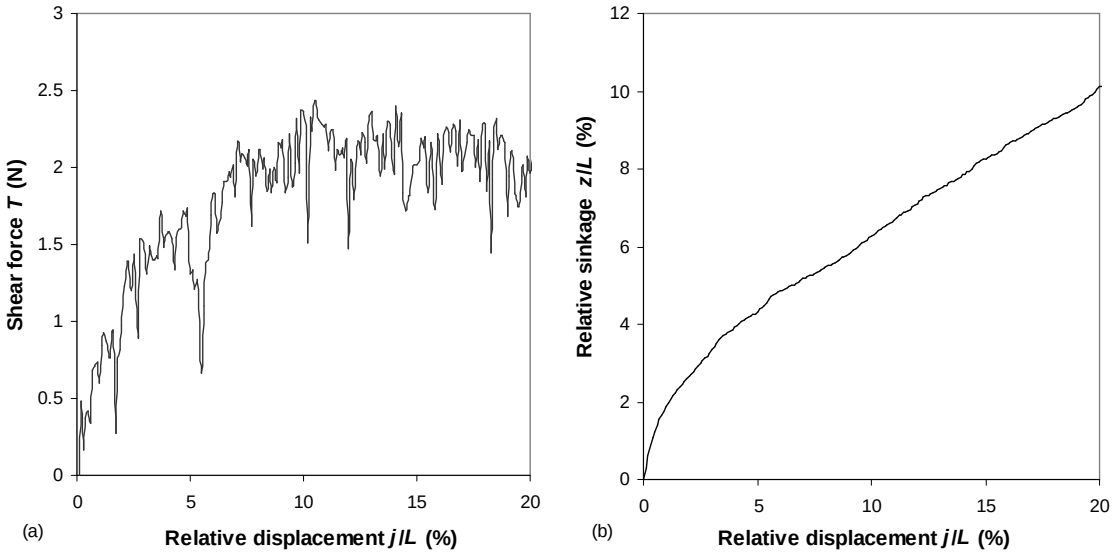

Figure 7. Numerical test (grousers, N = 5 N, fast speed), (a) (j/L, T) curve, (b) (j/L, z/L) curve

One of the advantages of these DEM numerical models is that the failure mechanism can be visualized. This failure mechanism can be approximated by a located mechanism formed by juxtaposed and successive slip lines (Figure 8). This type of geometry makes it possible to define a simple analytical model. The shape of the failure zones depends on the interface of the shear plate. The smoother the interface is, the thinner the mobilized soil is.

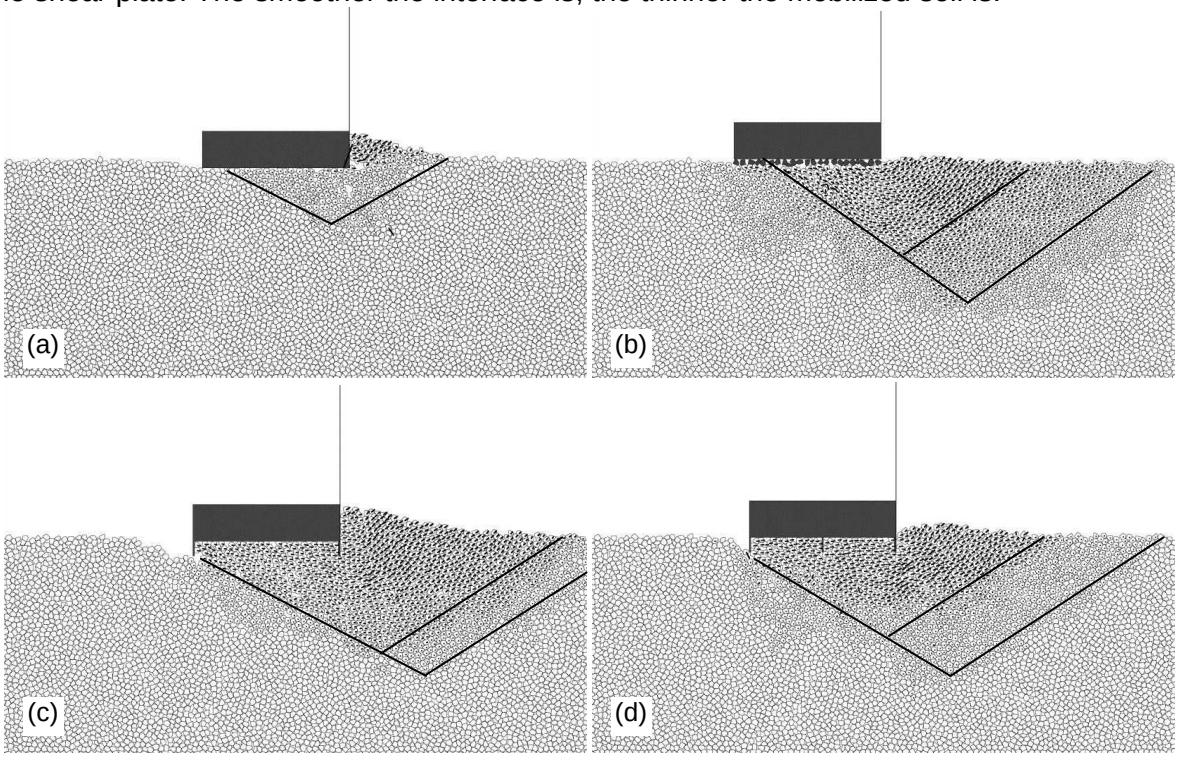

Figure 8. Failure mechanisms (a) smooth plate, (b) rough plate, (c) plate with two grousers, (d) plate with three grousers

5. Modelling and Calculation of soil parameters

5.1. Equations of the problem

The failure mechanism can be analytically approached by geometry with two rigid blocks (Figure 9). This method, where blocks are widespread for stability calculations, is cinematically acceptable.

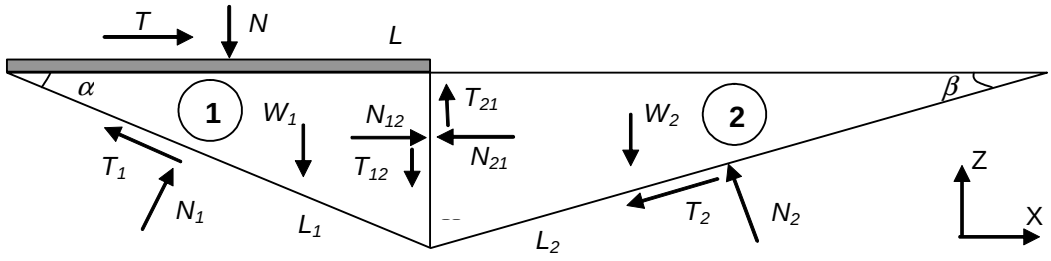

Figure 9. Failure mechanism with two rigid blocks

Using the identified geometry, the force balance can be put into an equation to carry out an ultimate equilibrium calculation, i.e. by assuming that the limit of soil resistance is reached along the lines. Solving the problem leads to a system of two equations with two unknown factors. The force balance provides a relation between forces N and T on the plate, the soil parameters γ, c and ϕ, and the geometrical parameters L, α and β. A parametric study is then possible with these parameters.

5.2. Parametric study

In order to evaluate the influence of each parameter compared to the others, a parametric study was carried out. Some parameters were fixed. The soil parameters were those of D1 sand: friction angle ϕ = 33°, null cohesion c, bulk unit weight γ = 16.3 kN.m^{-3}. The plate length L was 340 mm. Then the horizontal force T depended only on angles α and β and on the normal load N equal to 4.1, 8.2 or 12.3 kN. In comparison with the geometry of failure mechanisms observed in the numerical simulations, the assumption $\alpha = \beta$ was made. The experimental observations also confirmed the proximity between the values of the two angles.

The calculated forces T were compared with the experimental data (Figure 10). In D1 sand and for a normal load N = 4.1 kN (σ = 50 kPa), the value of the calculated force T was equal to experimental force T (T ≈ 1.9 kN) for an angle $\alpha = \beta$ = 11°. For the normal loads N = 8.2 kN and 12.3 kN (σ = 100 kPa and 150 kPa), this equality was found for an angle $\alpha = \beta$ = 18° with T ≈ 2.5 kN, and $\alpha = \beta$ = 22° with T ≈ 3.1 kN, respectively. All the values of angle α had a variation of more or less 3° because of the 6% variability Δ of the friction angle (31° < ϕ < 35°). The angle α between the failure line and the horizontal line increased with normal load N applied to the shear plate. The volume of the mobilized soil was then higher.

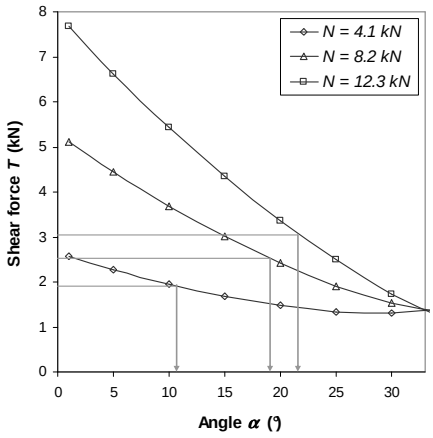

Figure 10. Determination of angle α for different normal loads N ($\alpha = \beta$)

The sinkage induced by soil shearing was observed in all the experimental tests and numerical simulations.

Two combined mechanisms caused this phenomenon. The first is a variation of the stress distribution below the plate involving a modification of the bulk unit weight of the soil. The displacement imposed during the translation shear test caused a soil breakage below and in front of the plate. This results in handling the soil and a loss of density in the upper layer. The plate applies a constant load and compacts the soil immediately below, whereas its displacement reworks the layer. The plate passes constantly from a dense medium to a less dense medium, causing a continuous sinkage. The scale of this sinkage is governed by the orientation of the slip surface under the plate, itself governed by normal load N.

The second mechanism is the sinkage of the plate depending on the failure line induced by its load (Figure 16). In the shear tests carried out on D1 sand, the sinkage induced by the horizontal displacement was quasi linear. In experiments, the shear plate followed a slip surface with an angle that can be evaluated with the measured sinkage (tan α = z/L).

The results of the calculations of the angle α (Figure 10) for various normal loads N highlight the similarity with the experimental data of the sinkage induced by shearing. The experimental values of the relative sinkage z_{100}/L for a normal load N of 4.1 kN, 8.2 kN and 12.3 kN were equal to 23%, 31% and 36%, respectively.

5.3. Calculation of the soil parameters

One of the advantages of shear tests is that they provide soil mechanics parameters and in particular the friction angle ϕ and the cohesion c used by the Mohr-Coulomb yield criterion. Calculating these parameters requires that the maximum shear stress on the failure surface be determined.

For a direct shear test, the failure surface is predetermined, horizontal and perpendicular to the load of the box. In this case, the measurement of the maximum shear force, to the peak state or to the critical state depending on the soil type, is divided by the failure surface to obtain a shear stress directly exploitable in the Mohr plan (σ, τ). This concept is not usable in the case of the translation shear test because the failure surface is not directly below the plate, as the numerical simulations demonstrate. In this type of test, the shear force T divided by the plate surface S does not correspond to the maximum shear stress. The T_m/S values show a linear behaviour but are not superimposed with the Coulomb straight line corresponding to the values of the D1 sand, $\phi = 33°$ and $c = 0$ (Figure 11).

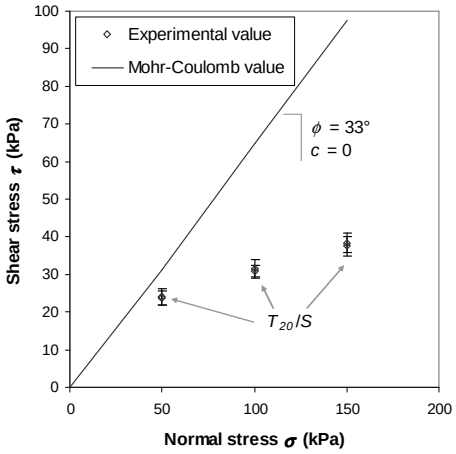

Figure 11. Experimental results and Coulomb straight line in the Mohr plan

The analysis of the failure mechanism provides a Mohr-Coulomb behaviour by locating the failure lines and therefore specifying the value of the maximum shear stress and calculating the soil parameters ϕ and c. This requires that the sinkage measured during the test to be used to calculate the angle α between the slip line and the horizontal. With this angle α and parameters T, N, γ, β, L, and c described previously, the friction angle ϕ of granular topsoil can be calculated using equilibrium calculation.

6. Conclusion

A prototype experimental device allows laboratory (and in-situ shear tests) by translation of a plate at slow or fast speed, representative of traditional soil mechanics tests and the real kinetics of the slip under a vehicle's running gear, respectively. The tests presented were performed in the laboratory on clean sand. The protocol to set up the soil allows a good reproducibility of the tests. The main results are: 1) the shear-displacement curves had no peak state so that the Janosi-Hanamoto approach could be used, 2) the tests showed a significant sinkage of the plate during the tests, 3) the increase in the translation speed induced a decrease in the initial slope of the curve and thus of parameter K of the Janosi-Hanamoto equation, 4) the critical state force was not modified by the speed, implying that the mechanical parameters (cohesion c and friction angle ϕ) were not affected by the translation speed in the range tested.

In order to visualize and understand the failure mechanisms involved in the translation shear test, simulations were performed using software based on DEM method. A failure mechanism located on juxtaposed and successive slip lines was identified. In a first approximation, an analytical approach of this mechanism related the geometry of the slip line

to the mechanical parameters of the granular soil. This approach is based on the method of calculation to the ultimate equilibrium for two rigid blocks.

Acknowledgments

The study presented was completed within the framework of research projects financed by the DGA of the French Defense Ministry.

Reference

1. Grima M., Delalance A., Sidoroff F., Cambou B., Jean M., Bohatier C., Gotteland Ph. Superficial soils: an attempt to model breaching, Proceedings of the 8th European Conference of the ISTVS, Umea, Sweden, pp. 17-24, 2000
2. Benoit O., Aptitude à la traficabilité des sols de surface remaniés aux engins chenillés: études expérimentales et modélisations phénoménologiques, PhD thesis (in French), Grenoble university, 2002
3. Aboura A., Etude expérimentale du comportement mécanique de matériaux granulaires non conventionnels, PhD thesis (in french), Grenoble university, 1999
4. Walker F.C., Hilf J.W., Daehn W.W., Holtz W.G., Wagner A.A., Gibbs H.J., Earth Manual, Bureau of Reclamation Denver, Colorado, 1954
5. Yong R.N., Youssef A.F., Fattah E.A., Vane cone measurements for assessment of tractive performance in wheel – soil interaction, Proceedings of the 5th International Conference of the ISTVS, Detroit, USA, 1975
6. Yong R.N., Hanna A.W., Finite element analysis of plane soil cutting, Journal of Terramechanics, vol.14, pp. 103-125, 1977
7. Bekker M.G., Off-the-road locomotion, the University of Michigan Press, Ann Arbor, 1960
8. Wong J.Y., Terramechanics and off-road vehicles, Elsevier, Amsterdam, 251 p., 1989
9. Upadhyaya S. K. , Wulfsohn D., Mehlschau J., An instrumented device to obtain traction-related parameters, Journal of Terramechanics, vol 30, n°1 , pp. 1 - 20, 1993
10. Bekker M.G., Theory of land locomotion, the University of Michigan Press, Ann Arbor, MI, USA, 1956
11. Reece A.R., The fundamental equation of earthmoving mechanics, Symposium on Earthmoving Mach. Auto. Div. Insts. Mech. Engrs., 1965
12. Oida A., Study on Equation of Shear Stress Displacement Curves, Report n°5, Farm Power and Machinery Laboratory, Hyoto University, 1979
13. Wong J.Y., Preston-Thomas J., On the characterization of the shear stress - displacement relationship of terrain, Journal of Terramechanics, vol.19, n°4, pp. 107-127, 1983
14. Janosi Z., Hanamoto B., The analytical determination of drawbar pull as a function of slip for tracked vehicles in deformable soils, Proceedings of the 1st International Conference on the Mechanics of Soil-Vehicle Systems, Edizioni Minerva Tecnica, Torino, Italy, 1961
15. Stafford J.V., Tanner D.W., Field measurement of soil shear strength and a new design of field shear meter, Proceedings of the 9th Conference of the ISTRO, Yugoslavia, 1982
16. Liston R.A., The combined normal and tangential loading of soil, Ph.D. Thesis, Michigan Technical University, Houghton, Michigan, 1973
17. Karafiath L.L., Nowatzki E.A., Soil Mechanics for Off-Road Vehicle Engineering, Trans Tech Publications, Clausthal, Germany, 1978
18. Benoit O., Gotteland Ph., DECART: Experimental device for trafficability characterization, Symposium International PARAM 2002, Paris, France, pp. 251-258, 2002
19. Benoit O., Gotteland Ph., Quibel A., Prediction of trafficability for tracked vehicle on breached soil: real size tests, Journal of Terramechanics, vol.40, Issue 2, pp. 135-160, April 2003
20. GTR 1992, Guide Terrassement Routier, Réalisation des remblais et des couches de forme, Fascicule I & II, SETRA, LCPC, D9233-1 & 2, 1992
21. Cundall P. A., Strack. O. D. L., A discrete numerical model for granular assemblies, Geotechnique, 29: 47-65, 1979
22. Jean M., *Frictional contact in collections of rigid or deformable bodies: numerical simulation of geomaterials*, Mechanics of Geomaterials Interfaces, Eds. A. P. S. Salvadurai & M. J. Boulon (Elsevier Science Publisher, Amsterdam), pp. 463-486, 1995
23. Moreau J. J., *Some numerical methods in multibody dynamics: application to granular material*, Eur. J. Mech. A/solids, Vol. 13 (4), pp. 93-114, 1994